

Membrane Environment Reduces the Accessible Conformational Space Available to an Integral Membrane Protein

Uwe Gerken,[†] Fedor Jelezko,[†] Britta Götze,[†] Marcus Branschädel,[‡] Carsten Tietz,^{*,†} Robin Ghosh,[‡] and Jörg Wrachtrup[†]

*Institute of Physics, University of Stuttgart, Pfaffenwaldring 57, D-70550 Stuttgart, Germany,
Institute of Biology, Department of Bioenergetics, University of Stuttgart,
Pfaffenwaldring 57, D-70550 Stuttgart, Germany*

Received: April 8, 2002; In Final Form: July 26, 2002

We studied the influence exerted on an integral membrane protein by its environment using the light-harvesting complex (LH1) of purple bacteria as a model. Single molecule spectroscopy of the LH1 bacteriochlorophyll pigments was used to compare membrane-reconstituted and detergent-solubilized complexes. The circular assemblies of the 32 bacteriochlorophyll *a* molecules present in the LH1 complex serve as a highly sensitive probe for protein deformation and disorder. It was shown that the membrane environment of the complex is essential for structural integrity, in particular, for conservation of the circular arrangement of pigments. We concluded that the membrane environment significantly narrows the statistical distribution of conformational states available to the LH1 complex in comparison to the corresponding state distribution observed for the same detergent-solubilized protein.

Introduction

In recent years, a number of integral membrane proteins have been solved by X-ray crystallography and cryoelectron-microscopy.^{1–6} Despite initial expectations, the amino acid packing density of all of these membrane proteins appears to be completely analogous to that observed for most water-soluble proteins and approximates that of amino acid crystals.⁷ These data were originally obtained predominantly from a very small sample membrane proteins solubilized in detergent micelles^{1–3} but have been confirmed also for membrane proteins determined more recently^{4–6} and would tend to preclude the possibility that the forces that stabilize membrane proteins and determine their conformational dynamics are peculiar to the membrane environment. This is in stark contradiction to the conclusions drawn from a large number of studies in the last 25 years, which have indicated that the properties of the membrane bilayer are crucial for membrane protein activity and stability.^{8–11} Indeed, early studies showed that membrane proteins are very often significantly less stable when isolated in detergent micelles than when present in the membrane, which has often been allocated to the effect of the significant lateral pressure observed when membranes are present in the liquid-crystalline (LQ) phase.¹² The importance of the LQ phase has been underlined by the many reports that a significant loss of membrane protein reconstituted into lipid bilayers with defined and physiologically accessible phase transition temperatures shows a loss of activity when the temperature is lowered to induce the gel phase. In the gel phase, it is known that only limited phospholipid dynamics occurs and the lateral pressure is low. This effect is commonly observed as a discontinuity in the activity vs temperature function when plotted in the Arrhenius representation.⁸ More recently, several short-time spectroscopic studies have shown that the coherent

nuclear motion of a typical integral membrane protein, the photosynthetic reaction center, is significantly affected when it is present in a membrane environment.^{13,14} Interestingly, the dampening of vibrational oscillations of the membrane-bound reaction center is reduced as compared to that of the detergent-solubilized form, which is completely consistent with the idea that rapid phospholipid dynamics observed in the LQ phase can influence membrane protein fluctuations.

In this study, we have employed single molecule fluorescence spectroscopy to examine the effect of the membrane environment upon the conformational dynamics of a model integral membrane protein, the light-harvesting 1 (LH1) complex from the photosynthetic bacterium *Rhodospirillum rubrum* without inlying reaction center. The LH1 complex, also designated here as B880 because of the absorption maximum of the Q_y transition, is particularly attractive for the spectroscopic study of conformational dynamics: (i) it is built from a simple repeating structure of two nonidentical polypeptides, α and β , containing 52 and 54 amino acids, respectively, which are associated as an $\alpha\beta$ heterodimer and binds two molecules of bacteriochlorophyll *a* (BChl *a*) and one molecule of carotenoid (spirilloxanthin, Spx);¹⁷ (ii) high-resolution cryoelectron microscopy has shown that 16 $\alpha\beta$ (BChl *a*)₂(Spx) are arranged in a ring-like structure which is embedded in a membrane;¹⁸ (iii) biochemical data has shown that both polypeptides traverse the membrane once and are oriented with their N-termini facing the cytoplasm;¹⁹ (iv) a single LH1 complex contains 32 BChl *a* pigments (Figure 1) and thus shows a very high fluorescence when excited in the near-IR region of the spectrum, thus providing a system with an exceptionally high S/N ratio; (v) biochemical procedures for the handling of *R. rubrum* LH1 complexes are now well worked out so that LH1 complexes can be reliably incorporated into membranes at extremely low LH1/phospholipid (PL) ratios.²⁰ Although a high-resolution structure of the LH1 at atomic resolution is not yet available, we have recently constructed a detailed model¹⁵ of the *R. rubrum* LH1 complex which can be perfectly accommodated within the EM projection

* To whom correspondence should be addressed. Phone: ++49/711/685-5231. Fax: ++49/711/685-5281. E-mail: c.tietz@physik.uni-stuttgart.de.

[†] Institute of Physics, University of Stuttgart.

[‡] Institute of Biology, University of Stuttgart.

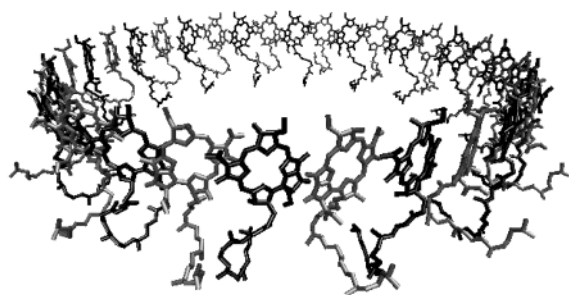


Figure 1. (A) Ring-like arrangement of the 32 BChl *a* pigments in the structure model of the LH1 complex.¹⁵ (Picture created by VMD.¹⁶)

data at 0.85 nm¹⁸ and that obtained recently at a resolution of 0.5 nm (P. Bullough and R. Ghosh, data not shown).

In this study, we have employed LH1 complexes from the carotenoid mutant, *R. rubrum* ST4,²¹ which contains the carotenoid 3',4',3,4-tetrahydrospirilloxanthin (thSpx) which is structurally identical to the wild-type complex but more stable to photooxidation. The LH1 complex have been purified to homogeneity and lack all traces of reaction center (RC).

Materials and Methods

We consider two well-defined physical states of the LH1 complex: (i) the LH1 complex solubilized in the short-chain phospholipid detergent, diheptanoyl-1,2,sn-phosphatidylcholine (DHPC) and immobilized on a mica surface (only in this detergent, so far, has it been possible to obtain a completely soluble form of the 32-fold symmetric LH1 complex without any significant fraction of subunits in a lower aggregation state);²² (ii) the LH1 complex reconstituted into membrane bilayers composed of the phospholipid dioleoyl-rac-phosphatidylcholine (DOPC) which has a phase transition temperature of -22 °C and is present in the liquid-crystalline phase at 6 °C, at which membrane protein reconstitution is largely performed.

LH1 complexes were obtained after purification as large aggregates present in vesicular-like structures containing 1–2 mol endogenous lipid/mol $\alpha\beta$ dimer.²⁰ The LH1 complexes were judged homogeneous and RC-free on the basis of their bulk spectral properties (absorption spectra, and near-IR circular dichroism spectra) and SDS–PAGE analysis. The aggregates were dissolved in 50 mM NH₄HCO₃ pH 7.8 (buffer A) containing 0.09% (w/v) DHPC and then mixed with preformed phospholipid vesicles of DOPC which had been presonicated with a microtip (Branson) at minimal power and allowed to equilibrate at room temperature for 10 min. The LH1-DHPC-DOPC mixture was then diluted 20-fold and centrifuged at 100 000 g to remove the excess DHPC, and the pellet was suspended in 1 mL of 50 mM NH₄HCO₃ pH 7.8. The suspended vesicles were then loaded onto a sucrose gradient (0.6–2 M) and centrifuged at 50 000 g for 22 h. After this time, the phospholipid band (containing reconstituted LH1 complexes) was isolated, diluted 20-fold, and centrifuged at 100 000 g for 1 h to remove excess sucrose from the LH1 membranes. The pelleted membranes were then suspended in 1 mL of buffer A and either used immediately or stored at 4 °C.

Membranes containing LH1 complexes incorporated at a molar ratio of 1 $\alpha\beta$ /4000 DOPC readily were adsorbed on mica surfaces and excited by a titan sapphire laser (Spectra Physics) at 865 nm. All measurements were performed using a home-built beam scanning-confocal microscope operating at 1.8 K. The samples were cooled to 77 K within milliseconds and subsequently to 1.8 K.

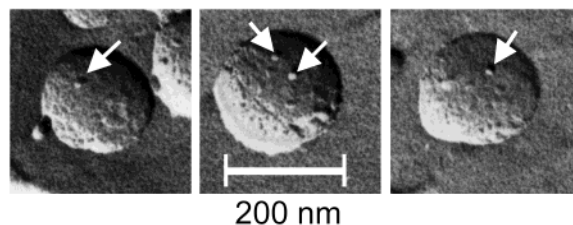


Figure 2. Freeze-fracture electron micrographs of LH1 complexes reconstituted into phospholipid vesicles. Arrows indicate isolated complexes. The magnification (100 000 \times) is indicated by a scale bar. The molar ratio of LH1 to phospholipid was 1:400. The complexes are well separated and show no aggregation.

The reconstitution of LH1 complexes into bilayer membrane vesicles was prepared as described previously for the preparation 2D crystals.²² As a further proof of reconstitution, we immobilized the vesicles on a mica surface and using fluorescence correlation spectroscopy (FCS) determined the diffusion constant to be $\bar{D} = 1.7 \times 10^{-9}$ cm²/s, consistent with expectation for membrane proteins of comparable size.²³

Results and Discussion

Freeze-fracture electron micrographs of membrane-reconstituted LH1 complexes at molar ratio of 1:400 (LH1 to phospholipid) showed that the complexes were well-separated from each other as shown in Figure 2 by the arrows. The molar ratio employed for the single molecule study here was 100-fold less than shown in Figure 2; that is, a molar ratio of 1:40 000 was used. It can be concluded that the probability having more than one LH1 complex per vesicle is extremely low, yielding the opportunity to expand investigations on other single pigment protein complexes^{24,25} to membrane-embedded complexes.

For the single molecule measurements, the reconstituted LH1 complexes in the liquid-crystalline state were frozen rapidly within milliseconds. Rapid freezing ensures that the transition to the solid state does not pass through the gel (L_β) phase.²⁶ Instead, the phospholipids are probably frozen in a disordered state corresponding to a “snapshot” of the liquid crystalline phase.

Only at low temperatures, it is possible to use the optical properties of the complex as a highly sensitive probe of structural deformation and disorder. This can be seen by considering the energy level diagram of the first excited state of the B880 ring (Figure 3A, left). For simulations, we used an effective Hamiltonian for Frenkel excitons in Heitler–London approximation for two level molecules without exciton–phonon coupling²⁷ as used by several groups to calculate the exciton states of LH2^{28–31} or LH1.³² With the exception of neighboring BChl *a* molecules, the distances between the pigments within the B880 ring are large enough to justify the point dipole approximation for calculating the coupling strength W_{ij} :

$$W_{ij} = C_3 \left(\frac{\vec{d}_i \cdot \vec{d}_j}{r_{ij}^3} - \frac{3(\vec{r}_{ij} \cdot \vec{d}_i)(\vec{r}_{ij} \cdot \vec{d}_j)}{r_{ij}^5} \right)$$

where d_i are unit vectors along the transition dipoles of the BChl *a* molecules and r_{ij} are the vectors connecting the Mg atoms of the BChl *a* molecules. For d_i , the direction from N_B to N_D atoms of the BChls was taken. All atomic positions were taken from a structure modeled for the LH1 of *R. rubrum* based upon the close sequence homology to the LH1 and LH2 $\alpha\beta$ peptides.¹⁵ Although the full details will be published elsewhere, briefly, the model was obtained as follows: first the conserved histidines in both apoproteins were assigned as the fifth ligand for a BChl

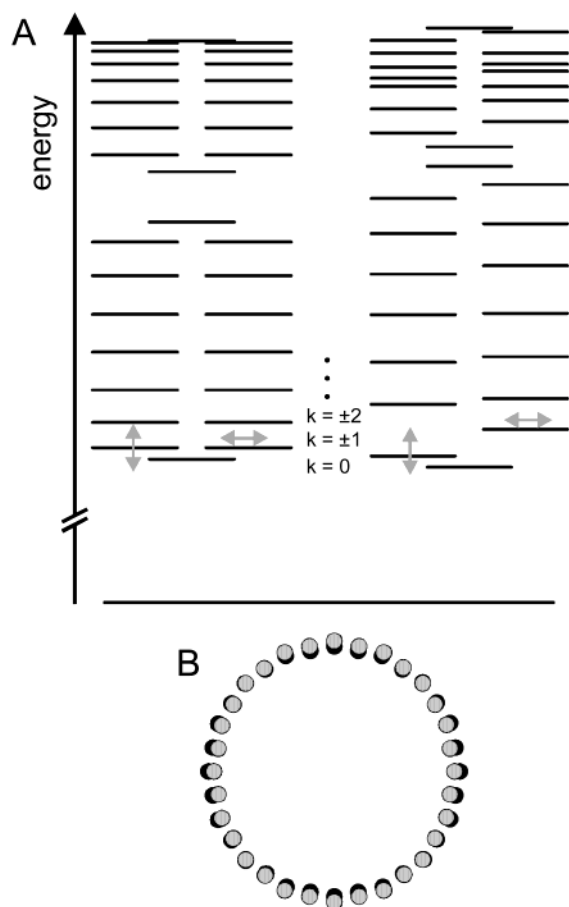


Figure 3. (A) Energy level diagram of undisturbed B880 ring (left) and elliptical deformed B880 ring using an eccentricity of $\epsilon = 0.32$ (right). The arrows indicate the directions of the transition dipole moments. (B) Schematic representation of the deformation. Black circles represent the circularly arranged BChl *a* molecules, and gray circles represent the BChls of the deformed ring.

a molecule each. Secondary structure was assigned with standard software and available physical data and the $\alpha\beta$ (BChl *a*)₂ dimer subjected to energy minimization. The minimized $\alpha\beta$ dimer was then arranged into a ring with 16-fold symmetry and the entire ring again energy-minimized.

The coupling strength between adjacent BChl *a* for LH2 was calculated using different algorithms leading to a relatively wide distribution of couplings between 200 and 800 cm⁻¹.^{29,33–37} (For a summary, see ref 38). Because of the close homology of the apoproteins of LH2 and LH1, it can be expected that the values for the coupling strength are comparable as well. Hence, we take $\nu_1 = 363$ cm⁻¹, $\nu_2 = 320$ cm⁻¹, and $C_3 = 348\,000$ Å³ cm⁻¹ obtained for LH2 of *Rhodospirillum rubrum*.³⁹ The parameters ν_1 and ν_2 are the coupling strengths for adjacent pigments (intra and interdimeric pigments, respectively) calculated using the collective electronic oscillator (CEO) approach.³⁹ From the coupling strength of the next but one pigments ($W_{13} = -102$ cm⁻¹, calculated by the CEO approach as well), C_3 is calculated using the above equation. C_3 is used for the coupling strength of all but adjacent pigments.

This strong coupling of the 32 BChl *a* molecules leads to 32 excitonic states which are delocalized over the whole B880 ring and numbered by the quantum number k of the translation operator. Because of the slight difference in coupling strength of BChl *a* molecules within a monomeric subunit and between monomeric subunits, these states are divided into two bands where all states except the lowest ($k = 0$) and highest ($k = 8$)

of both bands (Davidov components) show 2-fold degeneracy (see Figure 3A, left). For the case of perfect symmetry, the states $k = \pm 1$ carry almost all of the oscillator strength, whereas the lowest state $k = 0$ carries essentially no oscillator strength. However, every kind of disorder within the ring leads to both shifting of oscillator strength from the states $k = \pm 1$ to the other states and shifting of the energy levels. Fluorescence emission and excitation spectroscopy in dependence of the polarization of the excitation light yield the opportunity to measure the energetic positions of the states $k = 0, \pm 1$ and the orientation of the transition dipole moments. Beside from other optical properties, e.g., the line intensity and width, these are the most important properties to deduce the kind of disorder of the B880 ring.

At low temperatures ($T = 1.8$ K) in the first electronically excited state, only the lowest state ($k = 0$) of the manifold of exciton states is occupied. For the case of perfect symmetry, this would lead to a decrease and ultimately disappearance of the fluorescence with decreasing temperature. Nevertheless, from bulk measurements of LH1 solubilized in detergent, it is known that there is a slight increase of the fluorescence at low temperature.⁴⁰ It follows that the symmetry of the LH1 complex must be distorted in some way so as to shift the oscillator strength from the states $k = \pm 1$ to the state $k = 0$. This is also the case for single LH1 complexes embedded in membranes as well as solubilized in a detergent micelle. All LH1 complexes investigated showed a linearly polarized emission indicating the presence of only one emitting state. This could not only be explained by the observation of a single complex but also by strong coupled aggregates where the absorbed energy is exclusively transferred to one lowest state. The fact that we saw well isolated complexes in the freeze-fracture electron micrographs (Figure 2) renders the latter explanation extremely implausible.

Figure 4A,B shows typical emission spectra of single LH1 embedded in a membrane (Figure 4A) and inside a detergent micelle (Figure 4B). The former spectrum shows a clearly-resolved zero phonon line (ZPL) and a pronounced phonon wing, whereas in the spectra of detergent-solubilized LH1 complexes, it was not possible to resolve the ZPL because of the merging of the ZPL and the phonon wing. Additionally, a spectral shift between membrane-embedded LH1 complexes and detergent-solubilized complexes can be observed. Figure 4C shows two histograms of the spectral position of the ZPL or blue edge of the spectrum, respectively, for both 43 membrane-embedded complexes (green line) and 43 detergent-solubilized complexes (orange line). The maxima of the distributions are shifted by 5 nm in respect to each other. Though the pigments are bound to the same protein for both membrane-embedded and detergent-solubilized complexes, they show different solvent shifts. Hence, different environments of the LH1 complex show significant effects upon the protein environment of the pigments. Another difference between membrane-embedded and detergent-solubilized complexes is the missing of the ZPL in the emission spectra of the detergent-solubilized LH1. This behavior is due to differences in the amount of spectral diffusion which is much stronger in the case of detergent-solubilized complexes. It is known that minor conformational changes cause spectral diffusion within pigment protein complexes even at liquid helium temperatures.⁴¹ This spectral diffusion is most probably photoinduced such as shown for single LH2 complexes.⁴² In particular, the ZPL is extremely sensitive to minor changes of the protein environment, and therefore, slight differences of the protein conformation lead to different environments of the

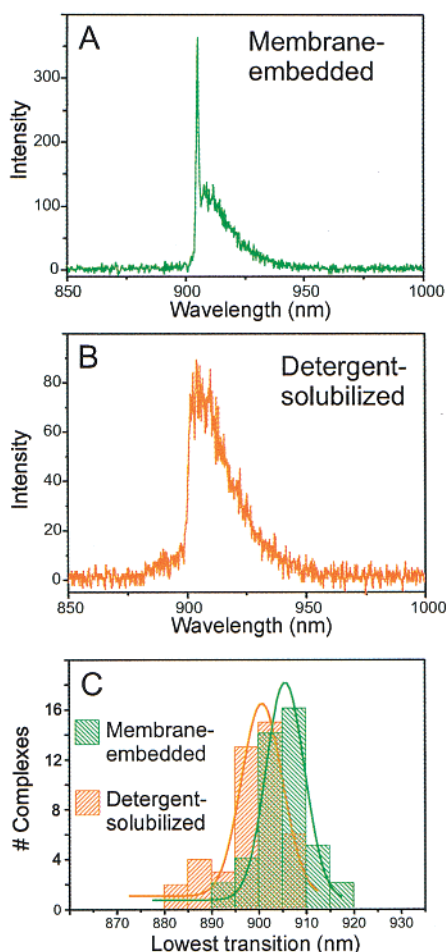


Figure 4. Fluorescence emission spectra of (A) membrane-embedded and (B) detergent-solubilized single LH1 complexes. Excitation wavelength was 865 nm. Because of high spectral diffusion in (B), the acquisition time was 10 times shorter than that used in (A). (C) Positional distribution of the ZPL (when resolved) and blue-edge (when the ZPL was not resolved), respectively, of the emission spectra from single LH1 complexes in different environments. The distributions are shifted by approximately 5 nm.

pigments and in turn to slight jumps in the optical spectra. The conformational changes are caused by the energy difference between the excitation and fluorescence photon which is dissipated within a single complex. Clearly, this leads to larger configurational changes of the protein structure in the case of detergent-bound complexes than in membrane-embedded complexes. For detergent-solubilized complexes, the conformational changes and in turn the optical jumps are so frequent during the acquisition of the emission spectra that no ZPL can be resolved. The membrane-embedded complexes on the other hand show only a few conformational changes that leads to changes in the optical spectra resulting in a more stable position of the ZPL.

The most striking difference between membrane-embedded and detergent-solubilized complexes can be deduced from fluorescence excitation spectra. Here, the excitation laser is scanned through the absorption bands of the first excited-state yielding a "single complex absorption spectrum" of the exciton manifold. A typical excitation spectrum from a single LH1 complex embedded in a membrane is shown in Figure 5A. Approximately 70% of all investigated membrane-embedded complexes exhibited comparable fluorescence excitation spectra (Figure 5C). The excitation light is linearly polarized, and the blue and red graphs represent two orthogonal directions of

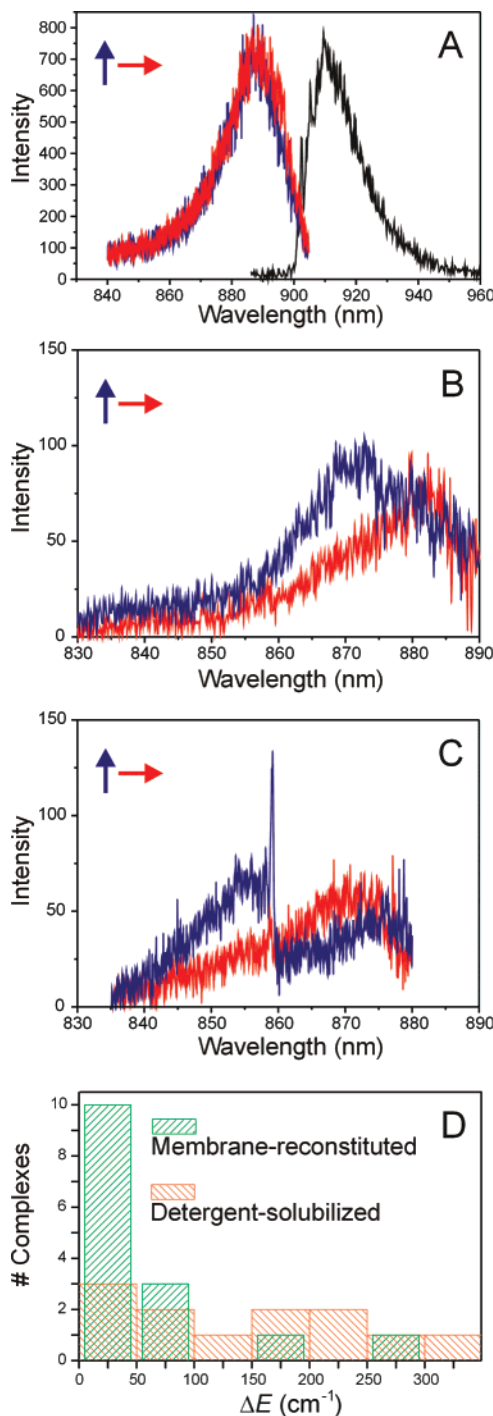


Figure 5. Fluorescence excitation spectra (red and blue) taken at orthogonal excitation polarizations of (A) membrane-embedded and (B and C) detergent-solubilized single LH1 complexes. Arrows indicate the directions of polarization. The black line in frame A represents the corresponding emission spectra. (D) Histogram of the splitting (ΔE) of the $k = \pm 1$ states for the membrane-embedded (green) and detergent-solubilized (orange) complexes.

polarization chosen from a sequence of six spectra where the direction of polarization was changed in 30° steps. Significantly, the spectra showed no dependence upon the polarization of the excitation light. For the case of an undisturbed or nearly undisturbed B880 ring, the states $k = \pm 1$ would be degenerate and carry almost the complete oscillator strength.

The fact that we only observe a single line in excitation spectra which is independent of the polarization, suggests that the states $k = \pm 1$ remain degenerate and that both states carry

nearly the same oscillator strength. From this behavior, two conclusions can be inferred for LH1 complexes within membranes: (i) the observation of fluorescence at low temperatures indicates the existence of a small configurational perturbation of the B880 ring of the complex causing a shift of oscillator strength from the states $k = \pm 1$ to the state $k = 0$; (ii) this perturbation does not manifest itself in a deformation of the entire ring, at least not in a perturbation which concerns the symmetry of the states $k = \pm 1$ because this would lead to a splitting of $k = \pm 1$ (see below) which is not observed. This behavior might be explained by a distribution of the energy eigenvalues of the 32 BChl *a* molecules (diagonal disorder) or by a distribution of the coupling strengths between adjacent BChl *a* molecules (nondiagonal disorder). Şener and Schulten⁴³ showed that the absorption spectra of light-harvesting systems are remarkably independent of the kind of disorder introduced. We used here a Gaussian distribution of the diagonal elements of the effective Hamiltonian to simulate the observed spectra. In practice, a moderate diagonal disorder of 150 cm⁻¹ and no additional deformation of the whole complex can be used to achieve the observed spectra. Such an moderate diagonal disorder yields an average splitting of the $k = \pm 1$ states of 24 cm⁻¹ and a standard deviation of 12 cm⁻¹. On the other hand, 30% of the investigated membrane-embedded complexes show a larger splitting which could be explained by additional distortions of the complex like discussed in the next paragraph for detergent-solubilized complexes.

These observations for membrane-embedded LH1 complexes differ significantly to those observed for detergent-solubilized complexes. In particular, the spectra of detergent-solubilized complexes exhibit two separated bands, which were linearly polarized and orthogonal to each other. A typical example is shown in Figure 5B where again the red and blue lines represent the two orthogonal directions of polarization of the excitation light. These two lines correspond to the states $k = \pm 1$ which are no longer degenerate. To calculate the splitting of $k = \pm 1$, each line was fitted by a Lorentzian line. The splitting ΔE of the lines is defined as the difference of the maxima of the Lorentzian lines. ΔE ranges from no splitting at all up to 300 cm⁻¹, and no further lines were found in the spectral range of shorter wavelengths. Interestingly, the spectral band in the blue region sometimes shows a proportionally narrow ZPL and a pronounced phonon wing (Figure 5C) comparable to that of the inverted emission spectrum (e.g., Figure 5A, black line). The line width of the ZPL is limited by the resolution of the laser used; that is, the corresponding energy transfer time is slower than 10 ps. Such long time components indicating a loss of structural integrity of the LH1 such that the BChl *a* pigments are partially decoupled have to our knowledge never been observed in ensemble investigations. Nevertheless, the fact that only two lines with orthogonal orientations appear in the excitation spectrum indicates that we are concerned here with the split states $k = \pm 1$. Both the large splitting of the states $k = \pm 1$ and the long energy transfer times indicate the existence of a strong ring distortion.

Nevertheless, the majority of detergent-solubilized complexes do not show narrow lines in the excitation spectra. In the following, the excitation spectra of these complexes should be simulated. For this, a model is needed which yields following properties: (a) splitting of the states $k = \pm 1$ up to $\Delta E = 300$ cm⁻¹, because the excitation spectra consist of two orthogonal lines; (b) no significant shift in oscillator strength of the states $k = \pm 1$ because the intensities of both lines are comparable; (c) no shift of oscillator strength to higher energy states because

no further lines at lower wavelength were found in the excitation spectra; (d) a slight shift of oscillator strength to the state $k = 0$ because this is the only occupied state of the exciton manifold at low temperatures and in turn, origin of the measured fluorescence.

To estimate the extent of this distortion which leads to a energy level scheme fulfilling these properties, we simulated energy level schemes containing several different distortions: (i) large diagonal disorder; (ii) deformation of the ring to a reduced C_2 symmetry;^{44,45} (iii) rupture of the B880 ring. (i) The large splitting values observed require the introduction of a diagonal disorder larger than 1000 cm⁻¹. However, this would lead to an additional shift in oscillator strength to higher states, which was not observed in the excitation spectra. (ii) A reduced C_2 symmetry can be obtained by an elliptical deformation of the whole complex. This leads to new positions and, consequently, to new couplings between the BChl *a* molecules. An important effect of the deformation is the fact that the distances between adjacent BChls are no longer constant over the ring; that is, it is not possible to use the constant couplings v_1 and v_2 . Instead, we used the point dipole approximation with slightly lower values for C so that in the limit of no distortion $W_{12} = v_1$ and $W_{23} = v_2$ hold. Hence, we obtain $C_1 = 192\,400$ Å³cm⁻¹ and $C_2 = 168\,800$ Å³cm⁻¹ for inter- and intradimeric coupling, respectively. As a measure for the deformation, the eccentricity is used, and a and b are minor and major elliptical axes:

$$\epsilon = \sqrt{1 - \left(\frac{a}{b}\right)^2}$$

Figure 3A shows the energy level diagram of the B880 ring for the undisturbed (left) and the elliptically deformed ring (right). Here an eccentricity of $\epsilon = 0.32$ was used. The change in position for the Mg atoms according to this eccentricity is shown in Figure 3B. The splitting of the states $k = \pm 1$ is approximately $\Delta E = 100$ cm⁻¹. A slightly larger deformation of the ring, for example, an eccentricity of $\epsilon = 0.50$, corresponds to a splitting of approximately $\Delta E = 250$ cm⁻¹. All higher states are only weakly influenced by the elliptical deformation. They remain quasidegenerate and obtain no measurable oscillator strength. (iii) To simulate a rupture of the B880 ring, we removed a few of adjacent BChl *a* molecules from the ring, whereas the rest of the ring remains unchanged. This causes only a small splitting of the states $k = \pm 1$. To achieve a splitting comparable to the experiment, additional, probably arbitrary changes of the coupling strengths in the remaining ring fragment would be necessary.

Whereas the first point (i) can be ruled out, it can only be speculated if one of the other points is the correct kind of distortion. For instance, van Oijen et al.⁴⁵ investigated detergent-solubilized LH2 (*Rhodospseudomonas acidophila*) complexes immobilized within a poly(vinyl alcohol) (PVA) matrix. In that work, the degeneracy of the states $k = \pm 1$ was lifted and a splitting on average of 110 cm⁻¹ was observed. This result was interpreted as a permanent distortion of the B850 ring, thereby reducing the C_9 symmetry to C_2 symmetry, which was suggested to be due to slight elliptical deformation of the entire ring. The observation of deformation of the ring in the case of LH1 complexes stabilized in a detergent micelle also observed for LH2 complexes,⁴⁵ and the absence of such a deformation in the case of LH1 embedded in a membrane reveals the significance of the environment for the structure and function of antenna complexes. Clearly, the bilayer environment is essential for stabilizing the whole LH1 complex in its highly symmetrical form. We note that the influence of the RC upon

the LH1 complex remains to be studied, as it is well-known that it is closely associated and immobilized by the LH1 complex both in vivo, as judged from photoselection studies,⁴⁶ as well as in vitro.²² Although the electron microscopy data suggest that the RC does not cause a fundamental change in the LH1 packing geometry,²² the resolution observable (about 1.3 nm) is for less than that obtainable for single molecule experiments. Thus, the question of whether the RC influences the LH1 symmetry will be the subject of a future study.

Finally, we believe that the results presented here are relevant to an understanding of the motional behavior of membrane proteins. For water-soluble proteins, it is usual to estimate the motional regimes of X-ray structure by means of the temperature-dependent B factors. Although the B factors contain contributions from both static lattice distortions as well as motional parameters of the polypeptide chain, the work of Karplus, Frauenfelder,⁴⁷ and others has shown that they are dominated by the latter. Generally, the B factors for water soluble proteins correlate with dynamic information obtained from high-resolution NMR studies of the same proteins in solution and thus yield motional information that is biologically relevant. For most membrane proteins available now at atomic resolution, the X-ray structures have been determined for detergent-solubilized forms. It is possible to argue that the single molecule experiments described here measure "snapshots" of fluctuating species contributing to bulk B factors. The fact that the population distribution of these "snapshots" in detergent differs from the membrane-embedded complexes implies that the bulk B-factors obtained from detergent-solubilized form should be treated with caution. This topic is worthy of further study.

Conclusion

The results presented above show that the membrane environment significantly narrows the statistical distribution of conformational states available to the LH1 complex, a typical integral membrane protein, in comparison to the corresponding state distribution observed for the same detergent-solubilized protein. The fluorescence excitation spectra obtained from the majority of membrane-bound complexes (70%) are strikingly similar to that obtained using bulk measurements, and the polarization data indicate that these complexes show predominantly radial symmetry, as deduced from the EM structural studies. We believe that these results show at the molecular level that the membrane environment makes a considerable contribution to the forces involved in stabilizing membrane protein structure and that dynamic information deduced from X-ray data temperature factors of detergent-solubilized membrane protein crystals should be treated with caution.

Acknowledgment. We thank the Volkswagen Foundation for financial support within the Priority Area "Physics, Chemistry and Biology with Single Molecules".

References and Notes

- (1) McDermott, G.; Prince, S. M.; Friend, R. H.; Hawthornthwaite-Lawless, A. M.; Papiz, A. M.; Cogdell, R. J.; Isaacs, N. W. *Nature* **1995**, *374*, 517–521.
- (2) Koepke, J.; Hu, X.; Muenke, C.; Schulten, K.; Michel, H. *Structure* **1996**, *4*, 581–597.
- (3) Kühlbrandt, W.; Wang, D. N.; Fujiyoshi, Y. *Nature* **1994**, *367*, 614–621.
- (4) Dutzler, R.; Campbell, E. B.; Cadene, M.; Chait, B. T.; MacKinnon, R. *Nature* **2002**, *415*, 287–294.
- (5) Palczewski, K.; Kumasaka, T.; Hori, T.; Behnke, C. A.; Motoshima, H.; Fox, B. A.; Le, T. I.; Teller, D. C.; Okada, T.; Stenkamp, R. E.; Yamamoto, M.; Miyano, M. *Science* **2000**, *289*, 739–745.
- (6) Lancaster, C. R. D.; Kröger, A.; Auer, M.; Michel, H. *Nature* **1999**, *402*, 377–385.
- (7) Rees, D. C.; Komiya, H.; Yeates, T. O.; Allen, J. P.; Feher, G. *Annu. Rev. Biochem.* **1989**, *58*, 607–633.
- (8) Cronan, J. E., Jr.; Gelmann, E. P. *Bacteriol. Rev.* **1975**, *39*, 232–256.
- (9) Carruthers, A.; Melchior, D. L. *TIBS* **1986**, *11*, 331–335.
- (10) Wiedmann, T. S.; Pates, R. D.; Beach, J. M.; Salmon, A.; Brown, M. F. *Biochemistry* **1988**, *27*, 6469–6474.
- (11) Moore, B. M.; Lentz, B. R.; Hoehli, M.; Meissner, G. *Biochemistry* **1981**, *20*, 6810–6817.
- (12) Seelig, J. In *Membranes and intracellular communication*; Balian, R., Ed.; Northern Holland publishing company: Amsterdam, The Netherlands, 1974; pp 17–78.
- (13) Vos, M. H.; Jones, M. R.; Hunter, C. N.; Breton, J.; Lambry, J. C.; Martin, J. L. *Biochemistry* **1994**, *33*, 6750–6757.
- (14) Vos, M. H.; Rappaport, F.; Lambry, J. C.; Breton, J.; Martin, J. L. *Nature* **1993**, *363*, 320–325.
- (15) Autenrieth, F.; Ritz, T.; Schulten, K.; Ghosh, R. **2002** submitted.
- (16) Humphrey, W.; Logunov, I.; Schulten, K.; Sheves, M. *Biochemistry* **1994**, *33*, 3668–3678.
- (17) Picorel, R.; Bélanger, B.; Gingras, G. *Biochemistry* **1983**, *22*, 2491–2497.
- (18) Karrasch, S.; Bullough, P. A.; Ghosh, R. *EMBO J.* **2000**, *14*, 631–638.
- (19) Meister, H. P.; Bachofen, R.; Semenza, G.; Brunner, J. *J. Biol. Chem.* **1985**, *260*, 16326–16331.
- (20) Ghosh, R.; Hoengger, A.; Mihailescu, D.; Hardmeyer, A.; Rosenbusch, J. P.; Engel, A. *J. Mol. Biol.* **1993**, *231*, 501–504.
- (21) Komori, M.; Ghosh, R.; Takaichi, S.; Hu, Y.; Mizoguchi, T.; Koyama, Y.; Kuki, M. *Biochemistry* **1998**, *37*, 8987–8994.
- (22) Stahlberg, H.; Dubochet, J.; Vogel, H.; Ghosh, R. *J. Mol. Biol.* **1998**, *282*, 819–831.
- (23) Cherry, R. J. *Biochim. Biophys. Acta* **1979**, *559*, 289–327.
- (24) Tietz, C.; Jelezko, F.; Gerken, U.; Schuler, S.; Schubert, A.; Rogl, H.; Wrachtrup, J. *J. Biophys. J.* **2001**, *81*, 556–562.
- (25) Jelezko, F.; Tietz, C.; Gerken, U.; Wrachtrup, J.; Bittl, R. *J. Phys. Chem. B* **2000**, *104*, 8093–8096.
- (26) Parente, R. A.; Höchli, M.; Lentz, B. R. *Biochim. Biophys. Acta* **1984**, *812*, 493–502.
- (27) van Amerongen, H.; Valkunas, L.; van Grondelle, R. *Photosynthetic Excitons*; World Scientific: River Edge, NJ, 2000.
- (28) Ketelaars, M.; van Oijen, A. M.; Matsushita, M.; Köhler, J.; Schmidt, J.; Aartsma, T. J. *J. Biophys. J.* **2001**, *80*, 1591–1603.
- (29) Hu, X.; Ritz, T.; Damjanovic, A.; Schulten, K. *J. Phys. Chem. B* **1997**, *101*, 3854–3871.
- (30) Sundström, V.; Pullerits, T.; van Grondelle, R. *J. Phys. Chem. B* **1998**, *103*, 2327–2346.
- (31) Matsushita, M.; Ketelaars, M.; van Oijen, A. M.; Köhler, J.; Aartsma, T. J.; Schmidt, J. *J. Biophys. J.* **2001**, *80*, 1604–1614.
- (32) Novoderezhkin, V.; Monshouwer, R.; van Grondelle, R. *Biophys. J.* **1999**, *77*, 666–681.
- (33) Sauer, K.; Cogdell, R. J.; Prince, S. M.; Freer, A.; Isaacs, N. W.; Scheer, H. *Photochem. Photobiol.* **1996**, *64*, 564–576.
- (34) Pullerits, T.; Hess, S.; Herek, J. L.; Sundström, V. *J. Phys. Chem. B* **1997**, *101*, 10560–10567.
- (35) Krueger, B. P.; Scholes, G. D.; Fleming, G. R. *J. Phys. Chem. B* **1998**, *102*, 5378–5386.
- (36) Scholes, G. D.; Gould, I. R.; Cogdell, R. J.; Fleming, G. R. *J. Phys. Chem. B* **1999**, *103*, 2543–2553.
- (37) Linnanto, J.; Korppi-Tommola, J. E.; Helenius, V. M. *J. Phys. Chem. B* **1999**, *103*, 8739–8750.
- (38) Tretiak, S.; Middleton, C.; Chernyak, V.; Mukamel, S. *J. Phys. Chem. B* **2000**, *104*, 4519–4528.
- (39) Tretiak, S.; Middleton, C.; Chernyak, V.; Mukamel, S. *J. Phys. Chem. B* **2000**, *104*, 9540–9553.
- (40) Monshouwer, R.; Abrahamsson, M.; van Mourik, F.; van Grondelle, R. *J. Phys. Chem. B* **1997**, *101*, 7241–7248.
- (41) den Hartog, F. T. H.; van Papendrecht, C.; Störkel, U.; Völker, S. *J. Phys. Chem. B* **1999**, *103*, 1375–1380.
- (42) van Oijen, A. M.; Ketelaars, M.; Köhler, J.; Aartsma, T. J.; Schmidt, J. *J. Biophys. J.* **2000**, *78*, 1570–1577.
- (43) Sener, M. K.; Schulten, K. *Phys. Rev. E* **2002**, *65*, 031916.
- (44) Bopp, M. A.; Sytnik, A.; Howard, T. D.; Cogdell, R. J.; Hochstrasser, R. M. *Proc. Natl. Acad. Sci. U.S.A.* **1999**, *96*, 11271–11276.
- (45) van Oijen, A. M.; Ketelaars, M.; Köhler, J.; Aartsma, T. J.; Schmidt, J. *Science* **1999**, *285*, 400–402.
- (46) Mar, T.; Picorel, R.; Gingras, G. *Biochim. Biophys. Acta* **1981**, *637*, 546–550.
- (47) Debrunner, P. G.; Frauenfelder, H. *Annu. Rev. Phys. Chem.* **1982**, *33*, 283–299.